VI International Conference on Computational Methods for Coupled Problems in Science and Engineering
COUPLED PROBLEMS 2015
B. Schrefler, E. Oñate and M. Papadrakakis(Eds)

DROP COALESCENCE SIMULATIONS USING LEVEL SETS COUPLED WITH BOUNDARY INTEGRAL METHODS

M. Garzon*, L. J. Gray† AND J. A. Sethian††

* Dept. of Applied Mathematics
Universidad de Oviedo
Calvo Sotelo s/n, 33007 Oviedo, Spain.
e-mail: maria.garzon.martin@gmail.com

† Bergen Software Services Int.,
Post Box 2921, 5852 Bergen, Norway.
e-mail:len@bssi-tt.com

†† Dept. of Math., U.C. Berkeley and Math. Dept., Lawrence Berkeley National Laboratory
1 Cyclotron Road, Berkeley, CA, USA
e-mail: sethian@math.berkekey.edu

Key words: Level Set Method, Boundary Integral method, Potential Flow, Drop Coalescence

Abstract. The study of singularities in free surface flows remains a subject of considerably interest. Regarding droplet dynamics the pinch-off events and merging of droplets have been extensively studied due its enormous interest in industrial applications. The level set techniques allows to embed the partial differential equations posed on a free boundary into one higher dimension equations posed on a fixed domain, in such a way that the classical potential flow model can be re-formulated in a complete Eulerian frame work, with the advantage that free boundary topological changes are automatically included. The Laplace equation for the velocity potential is solved via its integral formulation and a boundary element approximation, whereas the evolution of the level set function and extended velocity potential function is approximated using first order finite differences schemes. Merging and splitting events are therefore computationally possible. In the case of two equal drops coalescing, initial instants are very difficult to compute and also to see experimentally. After initial contact a liquid bridge connecting the two drops grows on time and a capillary wave, generated at the point of contact, propagates towards the drop end points. Numerical results regarding two droplet coalescence are presented and a detail discussion of the main flow characteristics is addressed. Comparison with previous computations and laboratory experiments will be also included.

1 INTRODUCTION

The phenomenon of coalescence entails a singularity in the free surface flow when the two liquid droplets initially touch and merge to form a single body. Understanding this complex flow is very important from both the theoretical view point as well as with regard to various industrial applications such as emulsion stability, cloud formation and nanofluidic technologies.

The general mathematical model to simulate this kind of flows is the Navier-Stokes equations but its complexity and computational cost have motivated the use of various simplifying assumptions. For low viscous fluids like water, the motion can be considered inviscid and irrotational up to length scales of few nanometers. One method for potential flow computation in moving and breaking domains, uses the level set embedding techniques to establish an Eulerian formulation of the classical Lagrangian equations [1, 2]. The advantage of this approach is that it seamlessly allows topologically breakup of droplets. It has proven to be a robust method in simulating various physical situations, such as wave overturning and breaking, see [1]; the Taylor-Rayleigh instability of a fluid jet, [2]; droplet and bubble evolution in a two fluid system, [3, 4]; and more recently electrical droplet deformation, [5].

In this paper we use the same model and numerical algorithm to simulate drop coalescence of two equal size droplets. In particular we analyze how our numerical method handles the onset of the singularity and the subsequent propagation of the surface capillary waves generated at the contact point. The evolution of the bridge radios is carefully studied to establish possible self similar solutions and scaling laws.

2 THE MODEL EQUATIONS

To introduce the model equations we follow the presentation in [2] and consider two time-dependent regions occupied by different fluids and separated by a moving boundary. We use the subscript F for the liquid and E for the exterior fluid. Let $\Omega_F(t)$, $\Omega_E(t)$ be three-dimensional moving fluid domains, $\Gamma(t)$ a parameterization of the free surface between both domains at time $t \in [0, T]$ and $\mathbf{R}(\mathbf{s}, t)$, $\mathbf{s} = (s_1, s_2)$ the position vector of a fluid particle on the moving front. See Fig. 1 for a 3D sketch of the physical domain.

We assume that the fluid in $\Omega_E(t)$ is at rest and p_a is the constant reference pressure. The fluid occupying $\Omega_F(t)$ is considered incompressible, irrotational and inviscid, and thus the conservation laws of mass and momentum in $\Omega_F(t)$ lead to the classical potential Eulerian-Lagrangian formulation:

$$\mathbf{u} = -\nabla\phi \quad \text{in } \Omega_F(t) \tag{1}$$

$$\Delta\phi = 0 \quad \text{in } \Omega_F(t) \tag{2}$$

$$D_t\mathbf{R} = \mathbf{u} \quad \text{on } \Gamma(t) \tag{3}$$

$$D_t\phi = f \quad \text{on } \Gamma(t), \tag{4}$$

where $\mathbf{u}$ is the velocity field, ϕ the velocity potential, p the pressure field and D_t stands

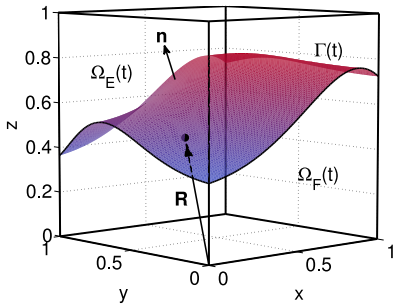

Figure 1: Schematic figure of the physical setting. $\Omega_F(t)$ is the fluid domain and $\Omega_E(t)$ is the exterior domain.

for the convective derivative, $D_t\phi = \frac{\partial \phi}{\partial t} + \mathbf{u} \cdot \nabla \phi$. The right hand side of Eqn. (4) is the function

$$f = -U + \frac{1}{2}|\mathbf{u}|^2 - \frac{p - p_a}{\rho}, \tag{5}$$

where the different terms represent the competing forces acting on the free boundary. Here ρ is the fluid density and U the potential function for the remainder of the body forces per unit mass in $\Omega_F(t)$. Depending upon the flow assumptions, some of these terms may be negligible compared to the others. For example, in the case of gravity wave propagation, see [1], the gravitational field $\mathbf{g} = -\nabla U$ has to be considered and surface tension forces can be neglected. Alternatively, the Rayleigh-Taylor instability and breakup of an infinite jet and the coalescence of liquid droplets are processes driven by surface tension and gravity terms can be neglected, see [2].

The pressure jump across the free surface $\Gamma(t)$ is therefore given by

$$p - p_a = \gamma \kappa \tag{6}$$

where κ is twice the mean curvature of the surface and γ the surface tension coefficient. Then equation 5 reads

$$f = \frac{1}{2}|\mathbf{u}|^2 - \gamma \kappa \tag{7}$$

Note that gravity forces have been neglected as inertia, surface tension are the dominant forces in the physical applications of drop coalescence presented here.

To make the equations dimensionless we introduce the usual characteristic scales for length r_0, capillary time t_0. The non-dimensional model equations remain the same except for f that becomes

$$f = \frac{1}{2}|\mathbf{u}|^2 - \kappa, \tag{8}$$

In what follows all the variables are dimensionless. We have thus avoided a separate notation for the dimensionless variables.

Next, we formulate the above Eulerian-Lagrangian equations in a complete Eulerian framework.

2.1 The Eulerian formulation of the model equations

Let Ω_D be a fixed three dimensional domain that will contain the free boundary for all times. In Fig. 1, $\Omega_D = \Omega_F \cup \Omega_E$. Eqns. (3) and (4), which are posed on a moving surface, can be reformulated in this fixed domain using the level set/extended potential technique described in [1, 2]. In this approach, the moving front $\Gamma(t)$ and velocity potential $\phi|_{\Gamma(t)}$ are embedded into functions Ψ and G of one higher dimension, respectively. The level set function Ψ and the extended velocity potential function G are defined on the fixed computational domain Ω_D that should contain the free boundary for $t \in [0, T]$ and such that

$$\Psi(\mathbf{R}(\mathbf{s}, t), t) = 0 \tag{9}$$

$$G(\mathbf{R}(\mathbf{s}, t), t) = \phi|_{\Gamma(t)} \tag{10}$$

for $t \in [0, T]$. Following the derivation in [2], Eqns. (3) and (4) transform into:

$$\Psi_t + \mathbf{u}_{\text{ext}} \cdot \nabla \Psi = 0 \quad \text{in } \Omega_D \tag{11}$$

$$G_t + \mathbf{u}_{\text{ext}} \cdot \nabla G = f_{\text{ext}} \quad \text{in } \Omega_D, \tag{12}$$

respectively. The subscript "ext" in Eqns. (11) and (12) denotes the extension of f and $\mathbf{u}$ onto Ω_D, the details of how to perform these extensions will be explained later. Note that we here have set $\Omega_D = \Omega_F \cup \Omega_E$, but it could be chosen in any other way. The only requirement is that the free boundary should always be included in Ω_D.

The Eulerian model equations for the coalescence problem are thus:

$$\mathbf{u} = -\nabla \phi \quad \text{in } \Omega_F(t) \tag{13}$$

$$\Delta \phi = 0 \quad \text{in } \Omega_F(t) \tag{14}$$

$$\Psi_t + \mathbf{u}_{\text{ext}} \cdot \nabla \Psi = 0 \quad \text{in } \Omega_D \tag{15}$$

$$G_t + \mathbf{u}_{\text{ext}} \cdot \nabla G = f_{\text{ext}} \quad \text{in } \Omega_D \tag{16}$$

$$\tag{17}$$

The rest of the boundary conditions and domain geometries have to be specified for each particular application.

The main advantage of the level set/extended potential formulation relies on the fact that any topological change of the free surface and evolving magnitudes within this boundary are directly taken into account by Eqns. (15) and (16). Moreover, the embedding provides a convenient regularization of possible singular geometries and prevents the blow up of diverging flow variables. This situation often occurs at fluid break-up and merging.

3 NUMERICAL APPROXIMATION

The time discretization is done using a explicit forward Euler scheme with time step Δt. At each time step t_n, given $\Psi^n = \Psi(t_n)$ and $G^n = G(t_n)$ the following semi-discretized system has to be solved:

$$\mathbf{u}^n = -\nabla\phi^n \quad \text{in } \Omega_F(t_n) \tag{18}$$

$$\Delta\phi^n(x,y,z) = 0 \quad \text{in } \Omega_F(t_n) \tag{19}$$

$$\phi^n|_{\Gamma_{t_n}} = G^n|_{\Gamma_{t_n}} \tag{20}$$

$$\frac{\Psi^{n+1}-\Psi^n}{\Delta t} = -\mathbf{u}^n_{\text{ext}} \cdot \nabla\Psi^n \quad \text{in } \Omega_D \tag{21}$$

$$\frac{G^{n+1}-G^n}{\Delta t} = -\mathbf{u}^n_{\text{ext}} \cdot \nabla G^n + f^n_{\text{ext}} \quad \text{in } \Omega_D. \tag{22}$$

Eqns. (18) to (20), which will be approximated using the Boundary element method, are strongly coupled to Eqns. (21) and (22), which are approximated by applying suitable finite difference level set schemes. First, the Dirichlet boundary condition (20) is obtained from the spatial mesh values of G^n in Ω_D and secondly $\mathbf{u}$ has to be provided from the boundary element calculation to yield $\mathbf{u}^n_{\text{ext}}$ and f^n_{ext} in the mesh points of Ω_D.

Regarding the spatial discretization, linear elements are used to discretize the free boundary and finite difference upwind schemes are used to approximate the level set equations (21), (22).

The basic algorithm can be summarized as follows:
For $n = 1, \ldots,$ number of time steps

1. Calculate $\mathbf{u}^n$ using the Boundary element method to solve Eqns. (19),(18).
2. Extend $\mathbf{u}^n$ on to Ω_D using the level set extension techniques.
3. Update Ψ at t_{n+1} using Eqn. (21) and the finite difference level set schemes.
4. Calculate the free boundary curvature κ^{n+1}
5. Calculate f^n as $f^n = \frac{1}{2}|\mathbf{u}^n|^2 - \kappa^{n+1}$.
6. Extend f^n on to Ω_D using the level set extension techniques.
7. Calculate G^{n+1} using Eqn. (22) and the finite difference level set schemes.
8. Interpolate G^{n+1} from the finite difference points to the boundary.

End For

4 DROP COALESCENCE SIMULATIONS

During coalescence of two drops of the same size they first touch and then merge as the liquid bridge connecting them grows in time. A capillary wave develops at the contact point and propagates away from the singularity. At early stages of the merging process the drop end points barely move, the dynamics occurs mainly in the bridge zone. Occasionally the capillary wave reaches the drop ends causing visible oscillations until the equilibrium state is finally achieved. For the numerical simulations presented here we take as initial geometry two spherical droplets of $r_0 = 1$ centered at $z = 0$ and $z = 2$, respectively, such that the initial contact point lies at $z = 1$. The fixed domain for the level set computations is set to $\Omega_D = [-1, 5, 3.5] \times [-1.5, 1.5]$ and the time span considered is $t \in [0, 1]$. A good practice to validate numerical results is to check for convergence with respect the discretization parameters. Simulations are run with (a) coarse and (b) fine grids with sizes:
(a) $\Delta r = \Delta z = 0.005$
(b) $\Delta r = \Delta z = 0.0025$.
To discretize the free boundary a high resolution is needed near the initial contact point, whereas at both ends of the droplet the size of the surface grid can be larger. We start with $\Delta s = 0.02$ near $z = 1$ and increase this distance gradually away from the center point using the regridding technique established in [2]. Therefore the number of points N_p to represent the free surface varies with time between $N_p = 141$ and $N_p = 135$. The time step is chosen adaptatively according with the criteria

$$\Delta t \leq \min(\frac{\Delta r}{|u_{\max}|}, 0.2\Delta s^{3/2}),$$

which leads to time steps as low as $\Delta t = 1. \times 10^{-5}$ to accurately resolve for the initial perturbation and can be increased to $\Delta t = 1. \times 10^{-3}$ once a steady neck growth is achieved.

A very challenging issue that remains open regarding full numerical computations is how to establish the initial conditions in the drop coalescence problem to avoid the singularity at $t = 0$. The general approach is to assume that immediately after the two free surfaces touch, a bridge of small but yet finite size already exists [6, 7, 8]. Another recent approach is to use the so called interface/disappearance model described in [9], which suppresses the initial singularity but entangles a much more complex mathematical model and the tuning of various model parameters. Within the present model and numerical framework, and due to the robustness of the level set method to handle topological changes, the initial condition is just two spheres touching tangentially at a single point and no artificial smoothing (besides the inherent to the discretization procedure) is needed. We do not claim the physical correctness of our initial contact evolution (molecular forces would probably play an important role) but just its computational simplicity, provided enough spatial-temporal resolution is given to resolve the small scales involved. We restrict ourselves to report the numerical results obtained which can be of interest to the computational community. In the present computations the early stages occur

Figure 2: Initial stage evolution: Reconnection event at $t = 0.00155$

in the time interval $t \in [0, 0.002]$, where the length of the contact line is stable or even diminishes with time. It is worthy to report that at $t = 0.00111$ and $t = 0.00155$ two free boundaries re-connections take place, hypothetically entrapping a thoroidal bubble of radius 5×10^{-5} non dimensional units, see a zoom of the area at $t = 0.00155$ depicted in Fig. 2. These events are easily handled by the level set technique and the computation proceeds smoothly.

Once the onset of the liquid bridge between the drops has taken place, how its minimum neck radios $r_{\min}$ evolves with time is a subject of interest, as theoretical works and experiments indicate the existence of certain scaling laws. Duchemin *et al* [6] established that, for inviscid fluids, capillary pressure should balance dynamical pressure at early stages of the process, that is $\rho(\frac{dr_{\min}}{dt})^2 \approx \Delta p$, from which the following scaling law is obtained:

$$r_{\min} \approx (\frac{\gamma R}{\rho})^{1/4} t^{1/2}$$

More recently, Paulsen *et al* [10] distinguished two different regimes regarding inviscid drop coalescence: an initial regime (never identified before) which they named the inertial-limited-viscous regime and a pure inertial regime. The scaling laws proposed by these authors are $r_{\min} \approx t$ and the above $r_{\min} \approx t^{1/2}$ respectively. They conclude that the initial regime should apply for drops of any viscosity. Nevertheless it is difficult to establish in which time range (or $r_{\min}$ range) these two regimes should apply due to the difficulty of obtaining reliable experimental or numerical data at such early stages of bridge formation.

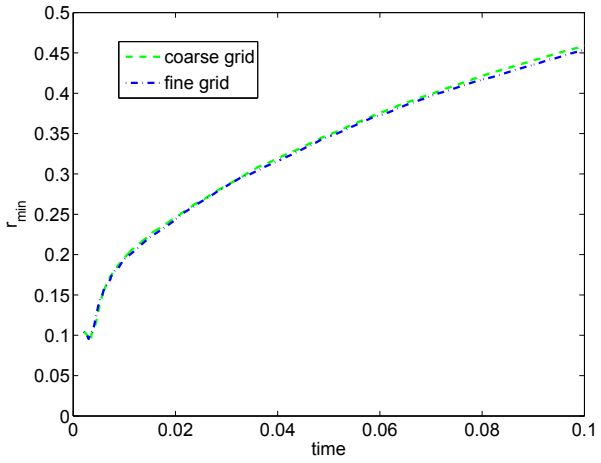

Figure 3: Minimum neck radios evolution

Therefore, one unavoidable characterization of the merging process is the time history of the minimum neck radios. In Fig. 3 we plot $r_{\min}$ versus t for both mesh sizes, from which we can conclude the independence of the results with respect the discretization parameters at the present refinement level. In what follows the numerical results correspond to the coarse grid. To check for the scaling laws proposed previously we plot in Fig. 4 $\log(r_{\min})$ versus $\log(t)$. Looking at this graph we can distinguish two very different slopes. A linear fit performed with Matlab gives an exponent of $\alpha = 1$ for very early times in $t \in [0.004, 0.007]$, and a very stable exponent of $\alpha = 0.4$ for times in the range $[0.018, 0.15]$ (and even beyond). The transition law between these two scaling laws would correspond to the theoretical $\alpha = 0.5$. The more persisting exponent of $\alpha = 0.4$ found in this work agrees very well with previously reported experimental results, see [8], [11], [7].

In Fig. 5 the evolution of the left end drop axial coordinate is depicted. As it can be observed from this graph, droplet deformation from $t \in [0, 0.4]$ is very much localized on the bridge region as the end points barely move. The capillary wave reaches these end points at around $t = 0.4$. In Fig. 6 we show the amplitude of the capillary wave with respect the superimposed initial condition at time $t = 0.1$. We have focused the capillary wave amplitude over the radial direction $y = x$. The amplitude of the wave with respect the sphere of $R = 1$ is approximately $4 - 5 \times 10^3$.

Drop profiles at selected times are depicted in Fig. 7. To compare our simulated results with the laboratory experiments in [11] we have to transform our non-dimensional times to dimensional ones multiplying by the characteristic time scale $t_o = \sqrt{\frac{\rho r_0^3}{\gamma}} = 1720 \mu s$. Here we have taken the usual water properties and $r_0 = 0.6$mm, which is the radios of the droplets in the experiments by Thoroddsen (see figure 12 of [11]). We observe that not only the drop profiles are in very good agreement with the experimental ones, but also the time occurrences.

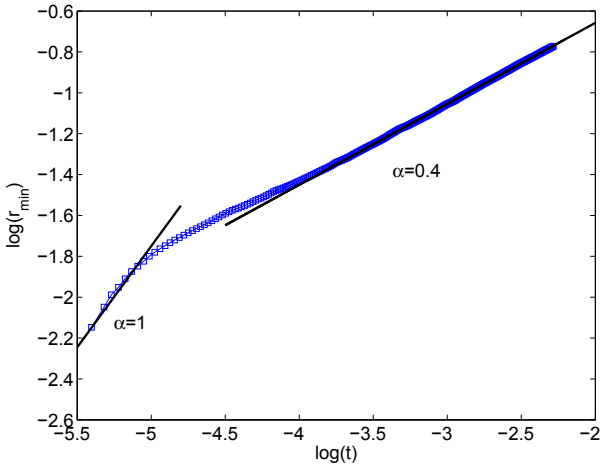

Figure 4: Log-log plot of minimum neck radios evolution

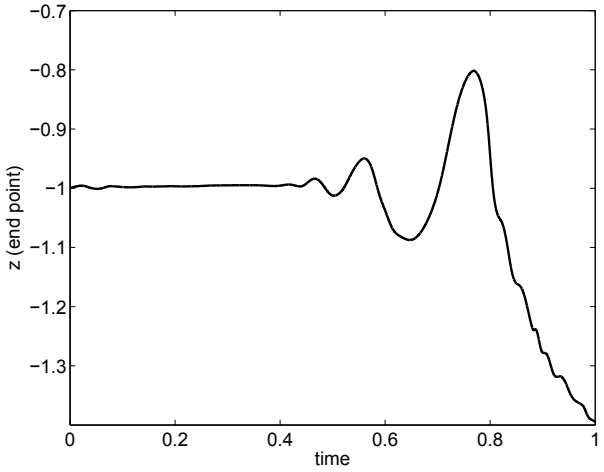

Figure 5: Left end drop axial coordinate evolution

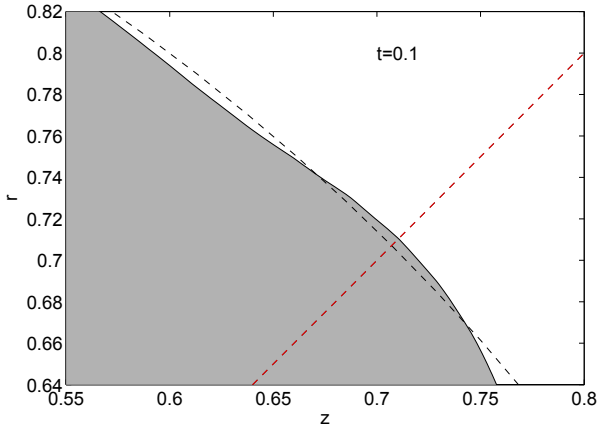

Figure 6: Capillary wave amplitude. Focused front and superimposed initial condition (dashed) at t=1. The dashed red line is the line $y = x$

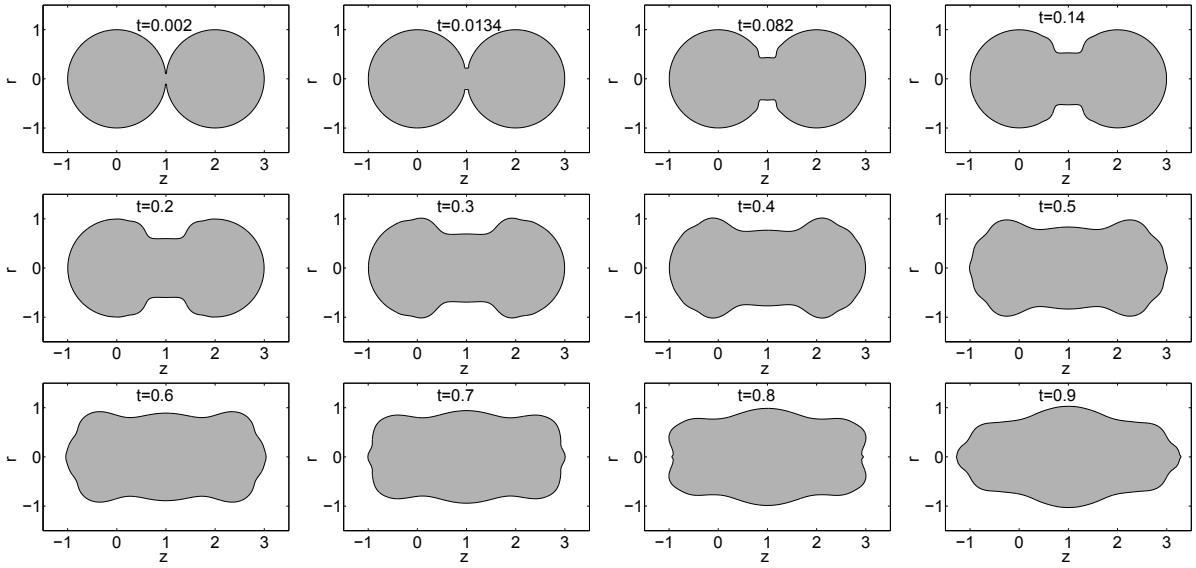

Figure 7: Fronts of two equal drops coalescing at indicated times

5 CONCLUSIONS

- In this paper we have used a three-dimensional algorithm with axial symmetry, based on the Boundary Integral-level set coupling to approximate hydrodynamic problems with free boundaries. Using the level set/extended potential model singular flow events, such as fluid break-up or merging, are easily handled and the computations can go past these singular times.

- In particular we have presented here the numerical results obtained in the case of two drops of same size coalescing. With our numerical technique there is no need to start the calculations with the artificial initial bridge needed in previous numerical simulations. Moreover, the scaling laws obtained, drop profiles and time occurrences are in very good agreement with published laboratory experiments.

REFERENCES

[1] Garzon, M., Adalsteinsson, D., Gray, L. J. and Sethian, J. A. A coupled level set-boundary integral method for moving boundary simulations. *Interfaces and Free Boundaries* (2005) **7**: 227-302.

[2] Garzon, M. and Gray, L. J. and Sethian, J. A. Numerical simulation of non-viscous liquid pinch-off using a coupled levelset-boundary integral method. *J. Comput. Phys.* (2009) **228**: 6079-6106.

[3] Garzon, M., Gray, L. J. and Sethian, J. A. Simulation of the droplet-to-bubble transition in a two-fluid system. *Phys. Rev. E* (2001) **83**: 046318.

[4] Garzon, M., Gray, L. J. and Sethian, J. A. Axisymmetric boundary integral formulation for a two-fluid system. *Int. J. Numer. Meth. in Fluids* (2012) **69**: 1124-1134.

[5] Garzon, M., Gray, L. J. and Sethian, J. A. Numerical simulations of electrostatically driven jets from nonviscous droplets. *Phys. Rev. E* (2014) **89**: 033011.

[6] Duchemin, L., Eggers, J. and Josserand C. Inviscid coalescence of drops. *J. Fluid Mech.* (2003) **487**: 167-178.

[7] Paulsen, J. D. *et all.* Coalescence of bubbles and drops in an outer fluid. *Nature Communications* (2014) **5**: 3182.

[8] Menchaca-Rocha, A., Martinez-Davalos, A., Nunez, R., Popinet, S. and Zaleski, S. Coalescence of liquid drops by surface tension. *Phys. Rev. E* (2001) **63**, 046309.

[9] Sprittles, J. E. and Shikhmurzaev, Y. D. Coalescence of liquid drops: Different models versus experiment. *Physics of fluids* (2012) **24** 122105.

[10] Paulsen J. D. *et al.* The inexorable resistance of inertia determines the initial regime of drop coalescence *Proc. Natl Acad. Sci. USA* (2012) **109**: 68576861.

[11] Thoroddsen T. S., Takehara K.,Etoh T. G. The coalescence speed of a pendant and sessile drop *J. Fluid Mech.* (2005) **527**: 85-114.